Equilibrium and pre-equilibrium processes in the ^{55}Mn(^{6}Li,xp) and ^{57}Fe(α,xp) reactions

A.V. Voinov,[1,*] S.M. Grimes,[1] C.R. Brune,[1] A. Bürger,[2] A. Görgen,[2]
M. Guttormsen,[2] A.C. Larsen,[2] T.N. Massey,[1] S. Siem,[2] and C. Kalbach[3]

[1]*Department of Physics and Astronomy, Ohio University, Athens, OH 45701, USA*
[2]*Department of Physics, University of Oslo, N-0316 Oslo, Norway*
[3]*Physics Department, Duke University, Durham, NC 27708-0305, USA*

Spectra of outgoing neutrons and protons from the ^{6}Li+^{55}Mn reaction and protons from the α+^{57}Fe reaction have been measured with beams of 15 MeV ^{6}Li ions and 30 MeV α particles. These reactions proceed through the same ^{61}Ni nucleus at the same excitation energy, thus allowing the difference in reaction mechanism to be studied. It is shown that spectra from the first reaction measured at backward angles are due to emission from a traditional compound nucleus reaction, in which the intermediate nucleus has reached statistical equilibrium; the spectra from the second reaction contain a significant fraction of pre-equilibrium emission at all angles. Level density parameters of the residual nucleus ^{60}Co have been obtained from the first reaction. Both emission spectra and angular distributions have been measured for the second reaction. It was found that the pre-equilibrium component exhibits a forward-peaked angular distribution, as expected, but with a steeper slope than predicted and with an unusual slight rise at angles above 120°. The backward-angle rise is explained qualitatively by the dominance of the multi-step compound mechanism at backward angles.

PACS numbers: 21.10.Ma,24.60.Dr, 24.60.Gv,25.55.-e

I. INTRODUCTION

Understanding the pre-equilibrium reaction mechanism is one of the most challenging problems in nuclear reaction physics. The term "pre-equilibrium mechanism" refers to the process through which an incoming particle's energy is gradually redistributed among more and more nuclear degrees of freedom. Energy equilibration can be described as a chain of particle-hole excitations, where the particle and hole degrees of freedom are referred to collectively as excitons. As the exciton number increases, some particle-hole pairs will annihilate, and a state of full steady-state energy equilibrium is reached. An outgoing particle can be emitted at any stage during the equilibration process, and this is usually referred to as "pre-equilibrium" emission, whereas particle emission occurring after statistical equilibrium has been achieved is referred to either as equilibrium emission or particle evaporation. Including the pre-equililbrium mechanism in calculations helps in interpreting the observed enhancements of high energy particle emission compared to predictions based solely on statistical evaporation at the equilibrium stage. In reality, however, there is no sharp dividing line between the two stages, since equilibrium is approached very gradually.

The situation becomes complicated when calculating the energy and angular distributions of the emitted particles. Sometimes, especially in studying the spectroscopy of low-lying energy states in the residual nucleus, it is convenient to consider only direct reactions—those involving a single target-projectile interaction. Some direct reaction mechanisms are inlcuded in common pre-equilibrium models and others are not, nor is their universal agreement as to which mechanisms are included in which models. In some applications it is useful to further divide the pre-equilibrium component into two parts: multi-step direct (MSD) and multi-step compound (MSC). Here, however, it is important to recognize that the equilibrium component represents additional MSC cross section, even though it is typically calculated using traditional equilibrium models. The MSD/MSC division of the cross section is discussed later in connection with the interpretation of the experimental angular distributions.

Since the whole process is very complicated, there is still no unified theory describing all aspects of it within the same framework. Instead, there are several approaches describing each stage separately. For a review of this topic, see Ref. [1].

One factor hindering further development of the theories is the lack of experimental data, especially double-differential cross sections of outgoing particles. Most of the data are available for forward angles, and detailed angular distributions for backward angles are often lacking or have poor statistics. As a result, the most developed theories are those related to the first stages of the equilibration process. These have the largest cross sections and produce strongly asymmetric, forward-peaked angular distributions. Angular distributions at backward angles are still not well understood except for purely equilibrium reactions, for which they are symmetric with respect to 90° in the center-of-mass system.

Although the angular distributions (pre-equilibrium and equilibrium) for nucleon-induced reactions can be

*Electronic address: voinov@ohio.edu

reasonably well described with the purely phenomenological Kalbach systematics [2], there is a reported problem for α-particle-induced reactions, for which experimental angular dependencies are often steeper than indicated by the systematics.

The more general problem directly related to the study of pre-equilibrium processes is to determine the relative fractions of pre-equilibrium and equilibrium emission represented in experimental energy spectra. Such a separation is usually model dependent and relies on input parameters used in the Hauser-Feshbach compound nucleus reaction model. The most uncertain quantity is the level density, which strongly affects the shape of particle evaporation spectra. Therefore, the level density appears to be crucial for the separation of experimental spectra into their pre-equilibrium and equilibrium components.

In this work we study inclusive proton spectra from the ^{55}Mn(^{6}Li,xp) and ^{57}Fe(α,xp) reactions experimentally. These reactions proceed through the same ^{61}Ni intermediate nucleus, and our incident energies are chosen to produce it with very nearly the same excitation energy. We will show that the spectrum from the first reaction measured at backward angles can be considered entirely due to the compound nucleus (or equilibrium evaporation) mechanism, whereas a large fraction of the (α,xp) cross section is known to be due to pre-equilibrium processes. Therefore, by comparing proton spectra from these two reactions, the pre-equilibrium fraction in the latter reaction can be obtained in a nearly model independent way. In addition, the level density of the residual nucleus ^{60}Co can be obtained from the proton evaporation spectrum of the lithium-induced reaction, and our understanding of this reaction can be verified by simultaneously reproducing the (^{6}Li,xn) reaction using the same model calculations.

II. EXPERIMENTS

A. The ^{55}Mn(^{6}Li,xp) and ^{55}Mn(^{6}Li,xn) reactions

The inclusive proton and neutron spectra from the ^{6}Li+^{55}Mn reaction have been measured with a 15 MeV ^{6}Li beam from the tandem accelerator of the Edwards Accelerator Laboratory, at Ohio University. The protons have been registered with a ΔE-E telescope consisting two silicon detectors. Their thicknesses were 150 μm for the ΔE detector and 3500 μm for the E detector. The latter was able to stop protons with energies up to 28 MeV, which was sufficient to measure the proton spectrum up to its maximum energy of around 25 MeV. The telescope was placed at a laboratory angle of 150°, to reduce or eliminate the contribution from non-equilibrium mechanisms. Because of the stopping power of the ΔE detector, only protons with energies above about 7 MeV were registered. The low energy portion of the proton spectrum, with proton energies up to about 10 MeV, was measured with the charged-particle spectrometer [3], in which the energy and the particle type were determined by the energy deposited in 1500 μm Si detectors and the flight time for the 2 m flight paths between the target and the detector. The measurement was carried out at 157.5°. The absolute cross section was obtained from the known target thickness, the integrated beam current, and the solid angle of the detectors. The target for all of the ^{55}Mn measurements was a 1 μm thick manganese foil coated with a thin (10 nm) carbon foil. The background caused by the carbon layer has been determined from a separate experiment on a carbon target and found to be negligible.

The neutron spectrum was measured at 125° and 140° with the neutron time-of-flight spectrometer of the Edwards Accelerator Laboratory. The 5 m flight path and NE-213 liquid scintillators were used to determine the energy of the outgoing neutrons. Detector efficiencies were determined with the calibrated neutron spectrum from the ^{27}Al(d,n) reaction measured with 7.5 MeV deuterons [4]. The spectra at the two angles were identical to within their error bars and were averaged for comparison with model calculations.

B. The ^{57}Fe(α,xp) reaction

Protons from the 30 MeV α-particle-induced reactions on ^{57}Fe have been measured with the ΔE-E technique at the cyclotron laboratory of the University of Oslo. The ΔE-E telescope consisted of a 200 μm thick ΔE Si detector and a 5000 μm thick Si(Li) detector. It was rotated around the target to measure the angular distributions. Spectra were measured at nine angles: 30°, 45°, 70°, 90°, 104°, 120°, 135°, 150°, and 160° in the laboratory system. A separate 1500 μm thick silicon detector was placed at 45° to monitor the beam current by measuring elastically scattered α particles. The 1.7 mg/cm^2 thick ^{57}Fe target was enriched to 95%.

In order to obtain absolute cross sections, the angular dependence of the elastically scattered α particles was measured and scaled to the results of optical model calculations. Only three data points from forward angles were used for the scaling, because at backward angles inelastic α particles populating the first excited level of ^{57}Fe, at 14.4 keV, might contaminate the elastic-scattering peak. Different optical model parameters taken from the RIPL-2 compilation [5] were tested. The best parameters were found to be under number 9401 in the compilation. Figure 1 presents the scaled experimental points along with the results of the optical model calculations. The uncertainty in this scaling is mostly determined by the average deviation of the scaled experimental points from the calculated ones, which is about 8% in our case. Uncertainties due to counting statistics do not exceed 1%.

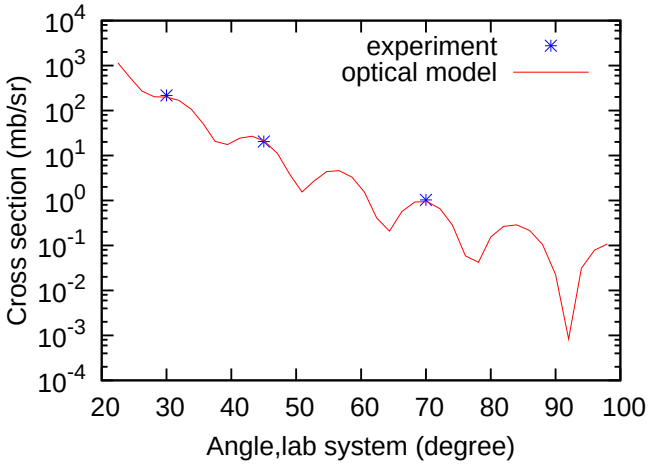

FIG. 1: The angular dependence of elastically scattered α particles. Points show the experimental data scaled to the calculation. Error bars due to counting statistics are less than the size of the points. The line show the results of calculations with the optical model potential N-9401 from the RIPL-2 database [5]

III. ANALYSIS OF EXPERIMENTAL SPECTRA

The experimental proton and neutron spectra from both reaction systems were converted to the center-of-mass system for comparison with calculations. The usual assumption that all particles were emitted from the fused target+projectile nucleus was made.

A. The ^{55}Mn(^{6}Li,xp) and ^{55}Mn(^{6}Li,xn) reactions

The proton and neutron spectra from the ^{6}Li+^{55}Mn reaction measured at backward angles have been analyzed with the EMPIRE computer code [6] using the Hauser-Feshbach compound-nucleus-reaction model [7] (see Fig. 2). No pre-equilibrium emission was allowed in the calculations, but sequential equilibrium emission of more than one particle was considered. Calculations were performed with two sets of model level densities. One was the Gilbert-Cameron composite formula [8], which uses a constant-temperature dependence at low energies and a Fermi-gas dependence at higher excitation energies, while the other was the microscopic model based on a statistical approach using the HF-BCS model [9]. Parameter systematics for the Gilbert-Cameron formula were taken from Ref. [10]. The Fermi-gas parameter a in the EMPIRE code is assumed to be energy dependent according to the Ignatyuk formula [11], which takes into account shell effects. The level density parameters for the residual ^{60}Co nucleus are as follows: the nuclear temperature T is 1.35 MeV, the adjustable energy shift E_0 is -3.39 MeV, the pairing energy Δ is 0.0 MeV, the asymptotic parameter $\tilde{a}$ is 7.95 MeV^{-1} and the parameter γ in the Ignatyuk formula is -0.054. We also tested the functional form of the original Fermi-gas (Bethe) formula [12] (without the constant temperature part) and found it to be totally consistent with the HF-BCS level densities for the residual nuclei populated in this reaction. We found that the experimental spectra are best reproduced with the Gilbert-Cameron formula, which includes the constant-temperature energy dependence at low excitation energies. Models using only the Fermi-gas energy dependence do not reproduce the shape of the evaporation spectra. This conclusion is in agreement with our previous results [13] and the results of Ref. [14], where the authors showed the importance of the constant-temperature level density in describing evaporation spectra in the $A = 50$ to 60 mass range.

We also compared results from the ^{55}Mn(^{6}Li,xp) proton spectrum with information from the ^{58}Fe(^{3}He,xp) reaction. The latter was measured with a 10 MeV ^{3}He beam, also at the Edwards Accelerator Laboratory [3]. In Fig. 3 we compare the experimental proton spectrum from the ^{3}He-induced reaction with Hauser-Feshbach calculations using the same Gilbert-Cameron level densities that were used to calculate the spectrum from the lithium-induced reaction (see Fig. 2). The conclusion is that the Gilbert-Cameron level density is able to reproduce the backward-angle proton spectra from both reactions.

The fact that proton spectra from both reactions are described with the same input level density function, even though the excitation energies in the intermediate nucleus were different, indicates the independence of the proton emission spectra on the type of projectile. We thereby conclude that at these incident energies, the dominant reaction mechanism at backward angles in both reactions and for all proton emission energies is particle emission from an energy-equilibrated compound nucleus.

B. The ^{57}Fe(α,xp) reaction

Proton spectra from the ^{57}Fe(α,p) reaction were measured at each of the nine experimental angles. The results are presented in Fig. 4, and the angle-integrated energy spectrum is shown in Fig. 5. An unusual feature of the data is the concentration of measurements at angles in the backward hemisphere with very good statistics (especially at 160 degrees) even at the higher emission energies, where the cross section is over two orders of magnitude lower than in the evaporation peak. This facilitates the study of the angular distributions at backward angles. The calculated spectra shown in Fig. 5 were obtained using the TALYS [15] and EMPIRE [6] computer codes. While both codes do well at reproducing the overall energy distribution of the emitted particles, TALYS uses the more sophisticated two-component exciton pre-equilibrium model and gives better agreement with the data, especially at the highest emission energies. Therefore we will use TALYS calculations to further analyze the

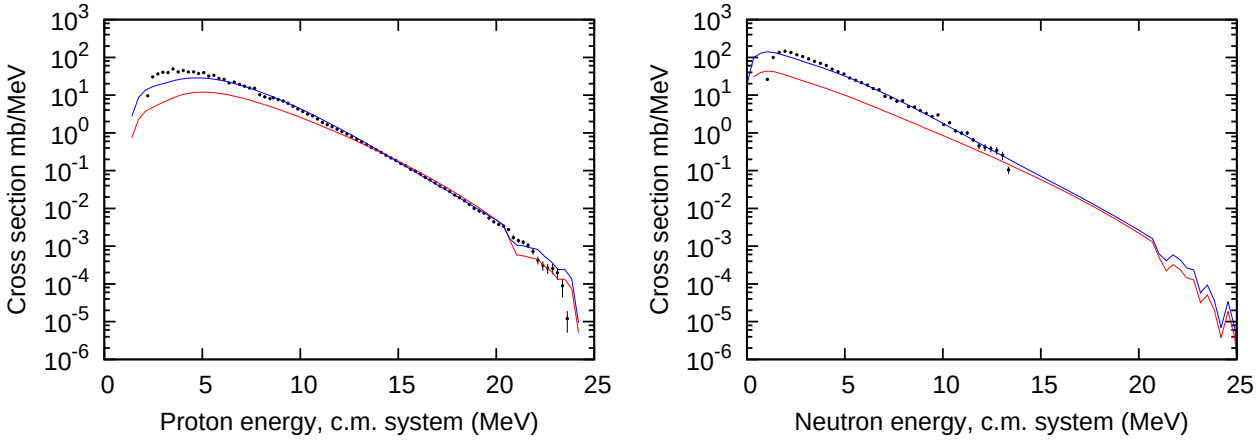

FIG. 2: Proton and neutron evaporation spectra from the ^{6}Li+^{55}Mn reaction. The points are experimental data taken at 157° for the lower proton energies and 150° for higher proton energies. The lines are the result of EMPIRE calculations with Gilbert-Cameron (top curve) and HF-BCS (bottom curve) input level density models. Experimental cross sections are multiplied by 4π sr to compare with the calculated, angle-integrated spectrum.

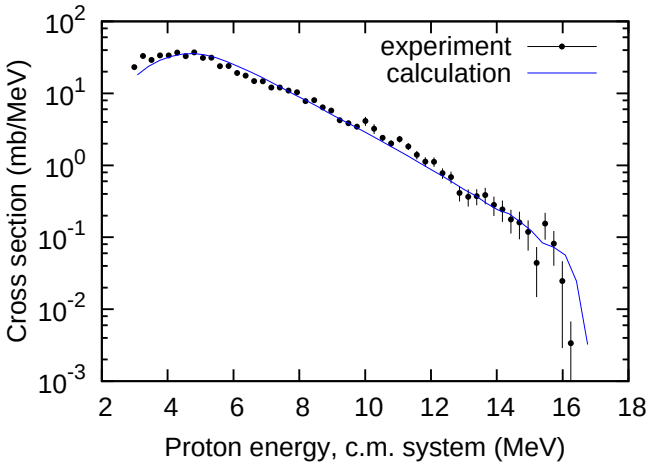

FIG. 3: The proton evaporation spectrum from the ^{3}He+^{58}Fe reaction. The points show the 157° data from Ref. [3] normalized to 4π sr, and the line shows the angle-integrated results of EMPIRE calculations using the Gilbert-Cameron level density model with the parameters from Ref. [10].

proton angular distributions. The small overall excess (25%) in the calculated cross sections relative to the experimental ones is well within the level of agreement one might expect from statistical models using a global input set. It can, in part, be explained by inadequacies in the level density parameters for the residual nuclei populated by the competing proton and neutron emission channels and/or by small contributions from direct processes not taken into account in the model calculations. Emission from the equilibrated compound nucleus was calculated with the input level density obtained from the ^{55}Mn(^{6}Li,xp) reaction, which thus forms a useful complement to the ^{57}Fe(α,xp) reaction.

The angular distributions for several energy bins of outgoing protons are presented in Fig. 6, along with the results of TALYS calculations. These calculations assume that the equilibrium component, calculated with the Hauser-Feshbach-model part of the code, is emitted isotropically. This is often a good approximation, but the emission is better described as being symmetric about 90° in the center-of-mass system, typically with a small dip or minimum at that angle. For the pre-equilibrium

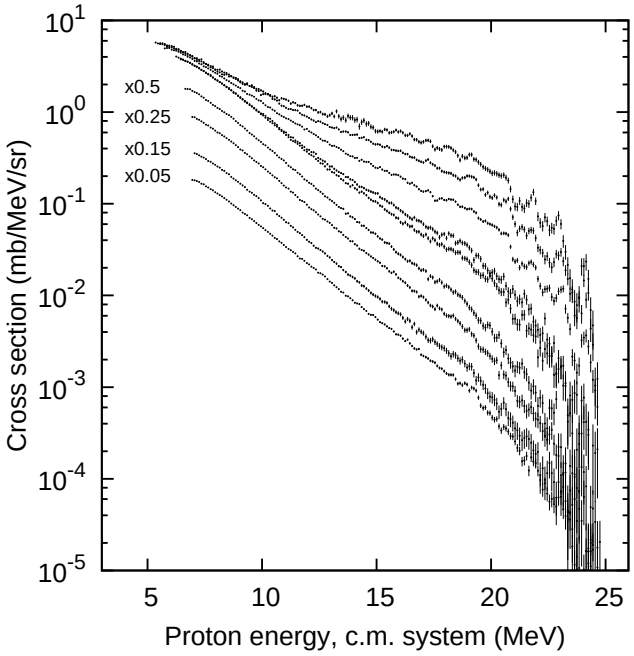

FIG. 4: Proton experimental spectra from the α+^{57}Fe reaction measured at laboratory angles of 30, 45, 70, 90, 104, 120, 135, 150, and 160 degrees (from top to the bottom). The four backward-angle spectra are scaled down for better visualization.

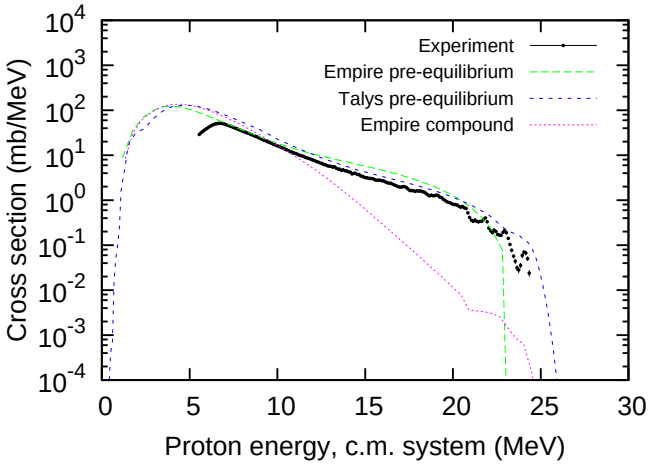

FIG. 5: The angle-integrated proton spectrum from the α+^{57}Fe reaction. The points show the experimental data, while the lines are the results of calulations using the EMPIRE and TALYS codes. The curves labeled "pre-equilibrium" also include contributions from the equilibrium or compound component.

component, TALYS uses the phenomenological Kalbach angular-distribution systematics [2]. These systematics are based on experimental results for a wide variety of reaction channels. Figure 6 shows that for low-energy outgoing protons, the experimental angular distributions are flat, and their near-symmetry about 90 degrees indicates

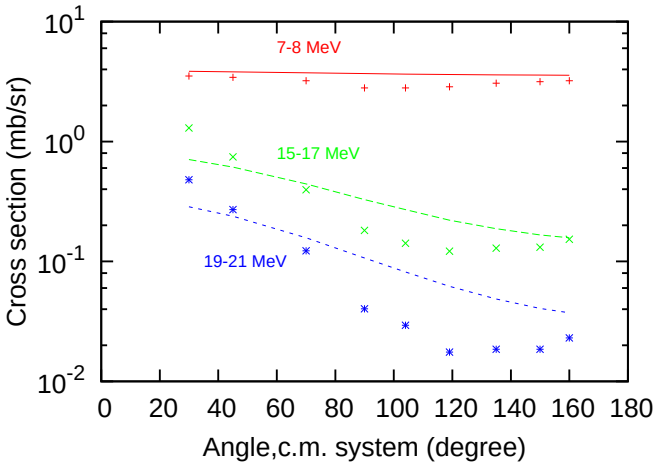

FIG. 6: Angular distribution of outgoing protons from different energy intervals. The points show the experimental results from the ^{57}Fe(α,xp) reaction, and the lines are from the calculations with the code TALYS.

that evaporation from the compound nucleus is the dominant reaction mechanism. Because of the assumption of isotropic emission for the equilibrium component, the calculations show much less of a dip around 90° than the data but otherwise give reasonable agreement with them. For more energetic protons, the equilibrium component decreases rapidly in intensity, and the angular distributions exhibit the forward-peaked behavior characteristic of pre-equilibrium processes. These angular distributions are not well reproduced by the TALYS results, which are much less forward-peaked than the data and fail to show the flat or slightly increasing cross section at angles above 120°.

To better understand this discrepancy between experiment and the Kalbach angular-distribution systematics used in the model calculation, it is useful to try to divide the measured cross section into its equilibrium and pre-equilibrium components. Fortunately, this is possible because the equilibrium component can be calculated based on the data from the ^{55}Mn(^{7}Li,xp) reaction. Figure 7 compares the experimental 160° proton spectrum with the equilibrium component calculated by TALYS. By subtracting the equilibrium component from the experimental spectra at each angle, the double-differential cross sections and thus the angular distribution of the experimental pre-equilibrium cross section can be determined. The calculated evaporation component was normalized downward by about 20% to reproduce the data at low emission energies before doing the subtraction. Figure 8 shows the angular distribution of the resulting pre-equilibrium component from the ^{57}Fe(α,xp) reaction integrated over emission energies from 16 to 25 MeV, where pre-equilibrium emission is dominant and the subtraction is most accurate. If the pre-equilibrium component were pure MSD, as is assumed in the model calculations, then this angular distribution should continue to decrease

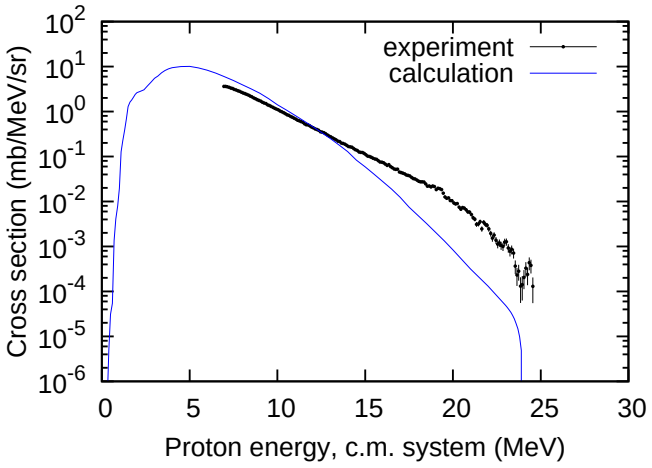

FIG. 7: Energy spectrum of outgoing protons from the ^{57}Fe(α,xp) reaction measured at a laboratory angle of 160^0. The points show the data, and the line is the compound nucleus reaction component calculated in the TALYS code.

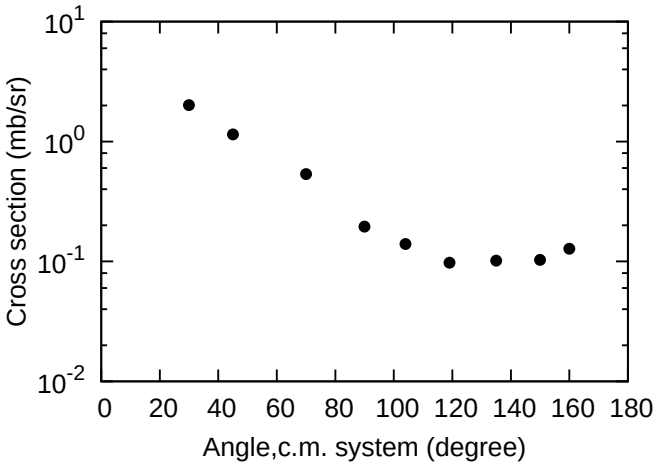

FIG. 8: Experimental angular distribution of pre-equilibrium outgoing protons with energies greater than 16 MeV from the ^{57}Fe(α,p) reaction.

with increasing angle. Instead it is again flat above 120°, with a small increase at 160°. The observed cross section at backward angles therefore implies that the pre-equilibrium component is not pure MSD but contains significant MSC pre-equilibrium cross section. This pre-equilibrium MSC cross section, because its angular distribution is symmetric about 90°, produces the observed rise in cross section at large angles in the figure. In this regard, it is interesting to note that the data from Ref. [16] showed a similar backward-angle rise in cross section for outgoing protons in the ^{56}Fe(α,xp) reaction at an incident energy of 23 MeV. All of this points to the need to reexamine the angular distribution systematics for the (α,xp) reaction channel, recognizing that some of the pre-equilibrium cross section will be multi-step compound in nature.

IV. IMPLICATIONS FOR THE KALBACH SYSTEMATICS

The Kalbach angular distribution systematics [2] utilize the division of the cross section into its multi-step direct (MSD) and multi-step compound (MSC) parts. Multi-step direct emission is defined as particle emission that occurs when the equilibrating nucleus has passed through a sequence of states all of which have at least one particle-degree-of-freedom in an unbound single-particle state [17]. It is made up of the direct and much of the pre-equilibrium cross section, and it exhibits a forward-peaked angular distribution described by an exponential in $\cos\theta$. Once the system passes through at least one configuration in which all of the particle degrees-of-freedom are in bound single-particle states, "memory" of the direction of motion of the projectile is assumed to be lost and the mechanism is termed multi-step compound. Subsequent particle emission is symmetric about 90° in the center-of-mass and contains exponentials in both $\cos\theta$ and $-\cos\theta$. The MSC cross section is composed of the rest of the pre-equilibrium component plus the equilibrium cross section. Thus, the systematics, when applied to equilibrium emision, avoid the assumption of isotropy used in TALYS and EMPIRE for that component.

The angular distribution of the double-differential cross section has the form

$$\frac{d^2\sigma}{d\Omega d\epsilon_b} = \frac{1}{4\pi}\frac{d\sigma}{d\epsilon_b}\frac{1}{e^{a_{\rm ang}}-e^{-a_{\rm ang}}}\left[(1+f_{\rm msd})e^{a_{\rm ang}\cos\theta} + (1-f_{\rm msd})e^{-a_{\rm ang}\cos\theta}\right] \quad (1)$$

where ϵ_b is the channel energy for the exit channel in the reaction, $f_{\rm msd}$ is the fraction of the cross section that is MSD, and $a_{\rm ang}$ is the angular distribution "slope parameter," used for both the forward-peaked MSD and symmetric MSC components. A slope parameter of zero would yield an isotropic angular distribution. The Kalbach systematics define the slope parameter as a function of the energies of the incident and emitted particles, and its values have been set phenomenologically, based on comparisons with a broad database.

In the later stages of developing these systematics and in their implementation in TALYS, it was assumed that the pre-equilibrium component is purely MSD. The comparison of experimental angular distributions with the systematics at 16 and 20 MeV (see Fig. 6), however, suggests that this assumption was inadequate and that the systematics need to be revised to be able to describe the data, especially at the higher emission energies where neither the amount of forward peaking nor the rise at backward angles is reproduced.

To quantify the problem, the experimental angular distributions from Fig. 6 were fit using Eq. (1) while varying the parameters $d\sigma/d\epsilon$, $f_{\rm msd}$, and $a_{\rm ang}$. The results,

shown in Fig. 9, demonstrate that the general form of the equation successfully reproduces the data. However the fitting process yields parameter values, summarized in Table I, which are quite different from the values from Ref. [2] used in TALYS. As expected, the slope parameters at 16 and 20 MeV are much larger than indicated by the Kalbach systematics. In addition, the values for $f_{\rm msd}$ at these energies are lower than $f_{\rm pre}$, the fraction of the cross section due to pre-equilibrium emission, obtained from TALYS. This confirms that there is likely to be an MSC contribution to the pre-equilibrium component. The fitted curves show that even a small amount of MSC cross section (6% to 7% at 20 MeV) can cause a significant rise in the cross section at backward angles when a large slope parameter causes the main, MSD part of the angular distribution to fall off rapidly with increasing angle. The existence of multi-step compound pre-equilibrium emission is known, but for nucleon-induced reactions it is most often concentrated in the region of the evaporation peak [18]. The enhanced MSC emission for high energy protons from α-induced reactions is a new result which needs to be understood.

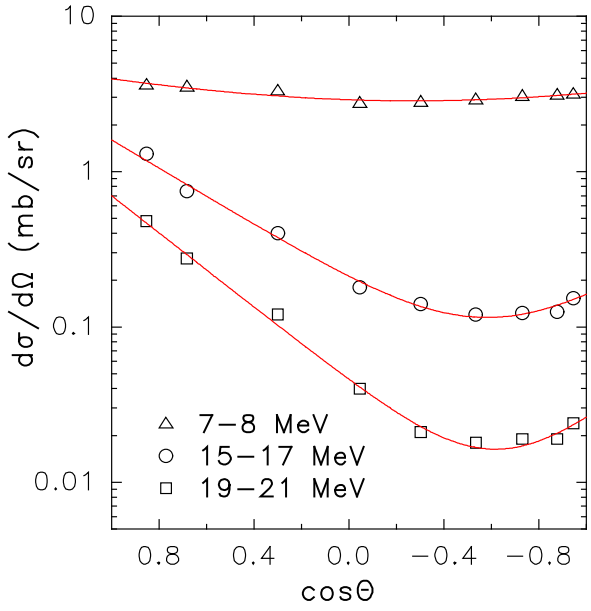

FIG. 9: Comparison between the experimental angular distributions for the ^{57}Fe(α,xp) reaction and the curves obtained by fitting using Eq. (1). The results are displayed as a function of $\cos\theta$ in order to show the exponential fall off of the cross section at forward angles at 16 and 20 MeV.

V. DISCUSSION

Physically, the results of the fitting process imply, for instance, that for 6% to 7% of the pre-equilibrium cross section for 20 MeV proton emission, the system has passed through one or more configurations where all the proton particle-degrees-of-freedom are in single particle states *below* the proton binding energy and that one such degree of freedom then gets promoted to a single particle state 20 MeV *above* the proton binding energy, through one or more two-body interactions. This kind of MSC pre-equilibrium emission is clearly possible, because we see equilibrium evaporation of such energetic particles, but detailed calculations in a single, unified framework will be needed to see if pre-equilibrium MSC emission can account for as much cross section as is indicated by fits to the data.

TABLE I: Comparison of parameters from fitting the experimental angular distributions with the parameters used in TALYS.

Proton energy	$a_{\rm ang}$ (sys.)	$a_{\rm ang}$ (fit)	sys/fit	$f_{\rm pre}$ (calc.)	$f_{\rm msd}$ (fit)
7.5 MeV	0.62	0.67(7)	1.1	0.05	0.18(3)
16 MeV	0.98	2.10(8)	2.1	0.90	0.84(1)
20 MeV	1.15	2.75(9)	2.4	0.99	0.935(6)

The probable presence of MSC pre-equilibrium cross section at such high emission energies (relative to the spectral endpoint) suggests that too much weight was given to backward-angle data (frequently with small cross sections and large error bars) in determining the slope parameters in the Kalbach systematics for α-particle-induced reactions, because that analysis assumed that pre-equilibrium particle emission was pure MSD. For α-particle induced reactions, the observed excess of forward-angle experimental cross section that was not reproduced by the resulting systematics was found in Ref. [2] to be qualitatively consistent with the observation of projectile-breakup fragments traveling with roughly the projectile velocity. However, a new preliminary model of light-projectile breakup [19] suggests that the breakup peaks should be less intense and have a narrower energy distribution than the excess cross section observed in Ref. [2]. This is again consistent with the need to reconsider the systematics for α-particle-induced reactions, putting more weight on intermediate and forward angles and less on the very backward angles.

VI. CONCLUSION

The proton spectra from both the ^{55}Mn(^{6}Li,xp) and ^{57}Fe(α,xn) reactions have been measured and compared with calculations performed using the exciton pre-equilibrium model and a Hauser-Feshbach evaporation model.

The backward-angle spectrum from the first reaction allows the level density parameters and the equilibrium component to be well determined, because the measured cross section appears to be almost exclusively due to particle evaporation from an energy-equilibrated system. Here it is found that the Gilbert-Cameron level density

model with the input parameters of Ref. [10] works well. This was confirmed by comparisons with earlier results on the ^{58}Fe(^{3}He,xp)^{60}Co reaction at 10 MeV.

The angular distributions from the ^{57}Fe(α,xp) reaction show two important effects. First, for emission energies above the main evaporation peak, the experimental cross section exhibits a significantly more rapid decrease with increasing angle than the calculated curves. This suggests that the Kalbach systematics for the (α,xp) channel and perhaps for all reactions with incident α-particles need to be revised. Second, the excellent data statistics in the backward-angle spectra (in particular the 160° spectrum) show a distinct flattening of the angular distributions and even a small rise in cross section at angles above 120° for the higher emission energies. Using the level-density parameters determined from the (^{6}Li,xp) reaction, it is shown that most of the cross section in this domain is not due to equilibrium evaporation of protons, so there are pre-equilibrium processes that exhibit a backward rise in cross section. This suggests that there is more multi-step compound cross section in the pre-equilibrium component at these energies than one might naïvely expect, especially given the predicted predominance of direct nucleon-transfer (stripping) reactions at proton energies of 16 and 20 MeV. This observation can help guide a re-evaluation of the angular distribution systematics for incident α particles.

VII. ACKNOWLEDGMENTS

We greatly acknowledge the help of D. Jacobs, D. Carter, J.O'Donnell for running the Edwards accelerator and for the computer and electronics support. We are also very grateful to E.A. Olsen and A. Semchenkov for running the Oslo Cyclotron. Financial support from the Research Council of Norway and U.S. Department of Energy grants numbers DE-FG52-06NA26187, DE-FG02-88ER40387, and DE-FG02-97ER41033 (Duke University, for C.K.) is greatly appreciated.

[1] E. Gadioli and P. E. Hodgson, *Pre-equilibrium Nuclear Reactions* (Clarendon Press, Oxford, 1992).
[2] C. Kalbach, Phys. Rev. **C37**, 2350 (1988).
[3] A. V. Voinov, S. M. Grimes, C. R. Brune, M. J. Hornish, T. N. Massey, and A. Salas, Phys. Rev. **C76**, 044602 (2007).
[4] T. N. Massey, S. Al-Quraishi, C. E. Brient, J. F. Guillemette, S. M. Grimes, D. Jacobs, J. O'Donnell, J. Oldendick, and R. Wheeler, Nucl. Sci. Eng. **129**, 175 (1998).
[5] T. Belgya, O. Bersillon, R. Capote, T. Fukahori, G. Zhigang, S. Goriely, M. Herman, A. V. Ignatyuk, S. Kailas, A. Koning, et al., *Handbook for calculations of nuclear reaction data: Reference input parameter library*, available at http://www-nds.iaea.org/RIPL-2/ (2005).
[6] M. Herman, R. Capote, B. Carlson, P. Obložinský, M. Sin, A. Trkov, H. Wienke, and V. Zerkin, Nucl. Data Sheets **108**, 2655 (2007).
[7] W. Hauser and H. Feshbach, Phys. Rev. **87**, 366 (1952).
[8] A. Gilbert, F.S.Chen, and A. Cameron, Can.J.Phys **43**, 1248 (1965).
[9] P. Demetriou and S. Goriely, Nucl. Phys. **A695**, 95 (2001).
[10] P. G. Young, E. D. Arthur, M. Bozoian, T. R. England, G. M. Hale, R. J. LaBauve, R. C. Little, R. E. MacFarlane, D. G. Madland, R. T. Perry, et al., Trans. Amer. Nucl. Soc. **60**, 271 (1989).
[11] A. V. Ignatyuk, G. N. Smirenkin, and A. S. Tishin, Sov. J. Nucl. Phys. **21**, 255 (1975).
[12] H. Bethe, Phys. Rev **50**, 332 (1936).
[13] A. V. Voinov, B. M. Oginni, S. M. Grimes, C. R. Brune, M. Guttormsen, A. C. Larsen, T. N. Massey, A. Schiller, and S. Siem, Phys. Rev. **C79**, 031301(R) (2009).
[14] R. Sherr and F. Brady, Phys. Rev. **124**, 1928 (1961).
[15] A. J. Koning, S. Hilaire, and M. C. Duijvestijn, in *Proceedings of the International Conference on Nuclear Data for Science and Technology (April 22-27, 2007, Nice, France)*, edited by O. Bersillon, F. Gunsing, E. Bauge, R. Jacqmin, and S. Leray (EDP Sciences, 2008), p. 211, URL `http://www.talys.eu/`.
[16] A. Alevra, M. Duma, I. R. Lukas-Koch, M. T. Magda, and M. E. Nistor, Nucl. Phys. **A265**, 376 (1976).
[17] H. Feshbach, A. Kerman, and S. Koonin, Ann.Phys. **125**, 429 (1980).
[18] C. Kalbach, Phys. Rev. **C33**, 818 (1986).
[19] C. Kalbach Walker (2010), report to the second Research Coordination Meeting of the FENDL-3 Coordinated Research Project of the International Atomic Energy Agency, URL `www-nds.iaea.org/fendl3/docs/dBreakupRCM2.pdf`.